CMES 中国机械工程学会
Springer Open
ISSN 1000-9345 · e-ISSN 2192-8258
CN 11-2737/TH · CODEN CJMEER

QK2146532

CHINESE JOURNAL OF MECHANICAL ENGINEERING®

Application of Digital Twin in Smart Battery Management Systems

Wenwen Wang, Jun Wang, Jinpeng Tian, Jiahuan Lu, Rui Xiong

DOI: 10.1186/s10033-021-00577-0

CJME

Vol. 34, No. 4
August 2021

万方数据

CONTENTS

Vol. 34, No. 4, August, 2021

CHINESE JOURNAL OF MECHANICAL ENGINEERING

Review

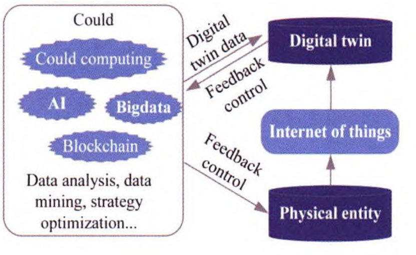

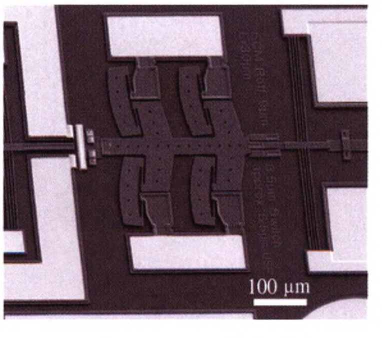

万方数据

CONTENTS

Vol. 34, No. 4, August, 2021

Intelligent Manufacturing Technology

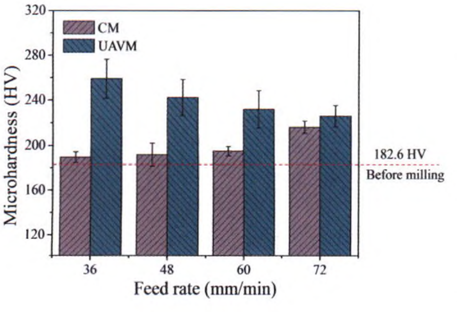

Abstract: The Ti6Al4V parts produced by the existing selective laser melting (SLM) are mainly confronted with poor surface finish and inevitable interior defects, which substantially deteriorates the mechanical properties and performances of the parts. In this regard, ultrasonically-assisted machining (UAM) technique is commonly introduced to improve the machining quality due to its merits in increasing tool life and reducing cutting force. However, most of the previous studies focus on the performance of UAM with ultrasonic vibrations applied in the tangential and feed directions, whereas few of them on the impact of ultrasonic vibration along the vertical direction. In this study, the effects of feed rate on surface integrity in ultrasonically-assisted vertical milling (UAVM) of the Ti6Al4V alloy manufactured by SLM were systemically investigated compared with the conventional machining (CM) method. The results revealed that the milling forces in UAVM showed a lower amplitude than that in CM due to the intermittent cutting style. The surface roughness values of the parts produced by UAVM were generally greater than that by CM owing to the extra sinusoidal vibration textures induced by the milling cutter. Moreover, the extra vertical ultrasonic vibration in UAVM was beneficial to suppressing machining chatter. As feed rate increased, surface microhardness and thickness of the plastic deformation zone in CM raised due to more intensive plastic deformation, while these two material properties in UAVM were reduced owing to the mitigated impact effect by the high-frequency vibration of the milling cutter. Therefore, the improved surface microhardness and reduced thickness of the subsurface deformation layer in UAVM were ascribed to the vertical high-frequency impact of the milling cutter in UAVM. In general, the results of this study provided an in-depth understanding in UAVM of Ti6Al4V parts manufactured by SLM.

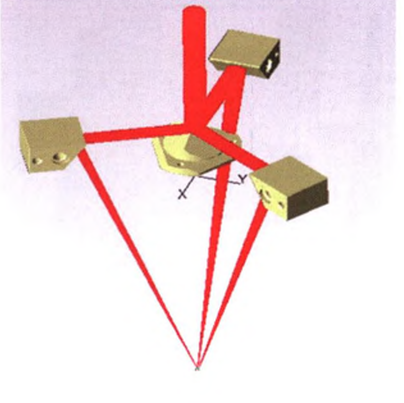

Abstract: Three-beam laser internal coaxial wire feeding cladding is regarded as a promising additive manufacturing technique because it is highly efficient and controllable. In this study, the effects of the defocus distance on cladding using a three-beam laser with internal wire feeding are experimentally and numerically studied. A process map indicating the surface characteristics at different defocus distances with various parameter combinations was developed. The transmission characteristics including laser intensity, beam size, and laser spot distance of the three-beam laser at different defocus distances were analyzed using TracePro software. Based on the TracePro results as heat source, a three-dimensional transient finite element (FE) thermal model was formulated to predict the thermal field, temperature history and molten pool shape at different defocus distances. A molten pool with a flat bottom and low melting depth is generated when the defocus distance is −2.5 mm, whereas when this distance is −1.5 mm, a pool with a valley-shaped bond and high melting depth is formed. The simulated results of the temperature cycle and clad geometry are both validated and found to well agree with experimental measurements. The influence of the defocus distance on the microstructure and microhardness are discussed based on the temperature history and cooling rate. With the increase in the absolute defocus distance, the height and dilution of the clad decreased, whereas the width increased. In addition, the effects of defocus distance with various parameter combinations on clad geometry were explored using the formulated FE model.

万方数据

(2021)34:43

DOI: 10.1186/s10033-021-00562-7

Studying Formability Limits by Combining Conventional and Incremental Sheet Forming Process

Fabio Andre Lora • Daniel Fritzen • Ricardo Alves de Sousa • Lirio Schaffer

Abstract: In this work it is assessed the potential of combining conventional and incremental sheet forming processes in a same sheet of metal. This so-called hybrid forming approach is performed through the manufacture of a pre-forming by conventional forming, followed by incremental sheet forming. The main objective is analyzing strain evolution. The pre-forming induced in the conventional forming stage will determine the strain paths, directly influencing the strains produced by the incremental process. To conduct the study, in the conventional processes, strains were imposed in three different ways with distinct true strains. At the incremental stage, the pyramid strategy was adopted with different wall slopes. From the experiments, the true strains and the final geometries were analyzed. Numerical simulation was also employed for the sake of comparison and correlation with the measured data. It could be observed that single-stretch pre-strain was directly proportional to the maximum incremental strains achieved, whereas samples subjected to biaxial pre-strain influenced the formability according to the degree of pre-strain applied. Pre-strain driven by the prior deep-drawing operation did not result, in this particular geometry, in increased formability.

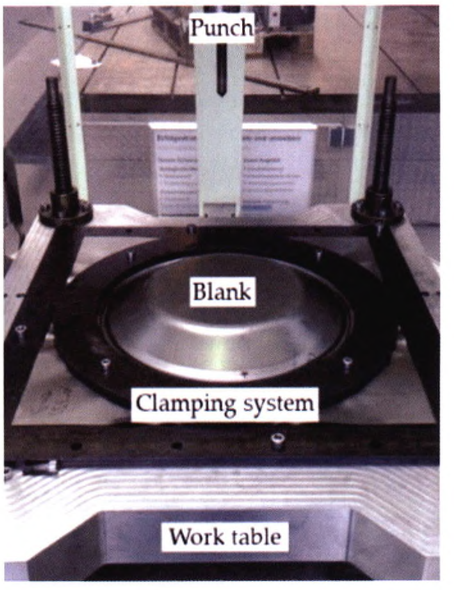

(2021)34:75

DOI: 10.1186/s10033-021-00593-0

Refill Friction Stir Spot Welding Al Alloy to Copper via Pure Metallurgical Joining Mechanism

Zhikang Shen • Yuquan Ding • Wei Guo • Wentao Hou • Xiaochao Liu • Haiyan Chen • Fenjun Liu • Wenya Li • Adrian Gerlich

Abstract: The current investigation of refill friction stir spot welding (refill FSSW) Al alloy to copper primarily involved plunging the tool into bottom copper sheet to achieve both metallurgical and mechanical interfacial bonding. Compared to conventional FSSW and pinless FSSW, weld strength can be significantly improved by using this method. Nevertheless, tool wear is a critical issue during refill FSSW. In this study, defect-free Al/copper dissimilar welds were successfully fabricated using refill FSSW by only plunging the tool into top Al alloy sheet. Overall, two types of continuous and ultra-thin intermetallic compounds (IMCs) layers were identified at the whole Al/copper interface. Also, strong evidence of melting and resolidification was observed in the localized region. The peak temperature obtained at the center of Al/copper interface was 591 °C, and the heating rate reached up to 916 °C/s during the sleeve penetration phase. A softened weld region was produced via refill FSSW process, the hardness profile exhibited a W-shaped appearance along middle thickness of top Al alloy. The weld lap shear load was insensitive to the welding condition, whose scatter was rather small. The fracture path exclusively propagated along the IMCs layer of Cu_9Al_4 under the external lap shear loadings, both $CuAl_2$ and Cu_9Al_4 were detected on the fractured surface on the copper side. This research indicated that acceptable weld strength can be achieved via pure metallurgical joining mechanism, which has significant potential for the industrial applications.

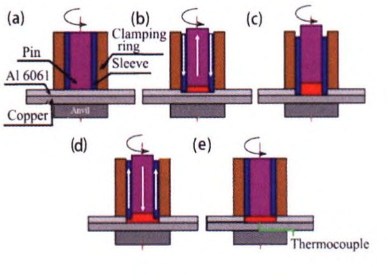

万方数据

CONTENTS

Vol. 34, No. 4, August, 2021

(2021)34:82
DOI: 10.1186/s10033-021-00603-1

Acoustics Based Monitoring and Diagnostics for the Progressive Deterioration of Helical Gearboxes

Kaibo Lu • James Xi Gu • Hongwei Fan • Xiuquan Sun • Bing Li • Fengshou Gu

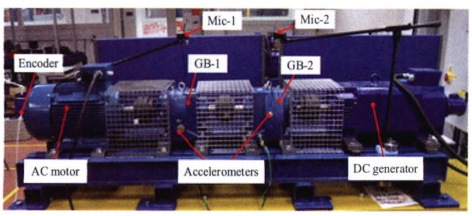

Abstract: Gearbox condition monitoring (CM) plays a significant role in ensuring the operational reliability and efficiency of a wide range of critical industrial systems such as wind turbines and helicopters. Accurate and timely diagnosis of gear faults will improve the maintenance of gearboxes operating under sub-optimal conditions, avoid excessive energy consumption and prevent avoidable damages to systems. This study focuses on developing CM for a multi-stage helical gearbox using airborne sound. Based on signal phase alignments, Modulation Signal Bispectrum (MSB) analysis allows random noise and interrupting events in sound signals to be suppressed greatly and obtains nonlinear modulation features in association with gear dynamics. MSB coherence is evaluated for selecting the reliable bi-spectral peaks for indication of gear deterioration. A run-to-failure test of two industrial gearboxes was tested under various loading conditions. Two omnidirectional microphones were fixed near the gearboxes to sense acoustic information during operation. It has been shown that compared against vibration based CM, acoustics can perceive the responses of vibration in a larger areas and contains more comprehensive and stable information related to gear dynamics variation due to wear. Also, the MSB magnitude peaks at the first three harmonic components of gear mesh and rotation components are demonstrated to be sufficient in characterizing the gradual deterioration of gear transmission. Consequently, the combining of MSB peaks with baseline normalization yields more accurate monitoring trends and diagnostics, allowing the gradual deterioration process and gear wear location to be represented more consistently.

(2021)34:63
DOI: 10.1186/s10033-021-00579-y

Magnetic Flux Leakage Course of Inner Defects and Its Detectable Depth

Jianbo Wu • Wenqiang Wu • Erlong Li • Yihua Kang

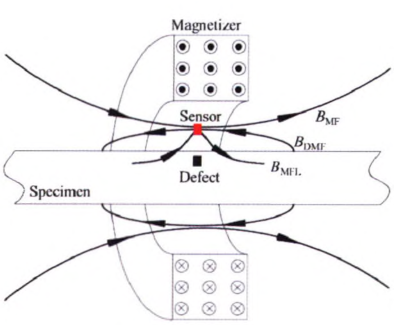

Abstract: As a promising non-destructive testing (NDT) method, magnetic flux leakage (MFL) testing has been widely used for steel structure inspection. However, MFL testing still faces a great challenge to detect inner defects. Existing MFL course researches mainly focus on surface-breaking defects while that of inner defects is overlooked. In the paper, MFL course of inner defects is investigated by building magnetic circuit models, performing numerical simulations, and conducting MFL experiments. It is found that the near-surface wall has an enhancing effect on the MFL course due to higher permeability of steel than that of air. Further, a high-sensitivity MFL testing method consisting of Helmholtz coil magnetization and induction coil with a high permeability core is proposed to increase the detectable depth of inner defects. Experimental results show that inner defects with buried depth up to 80.0 mm can be detected, suggesting that the proposed MFL method has the potential to detect deeply-buried defects and has a promising future in the field of NDT.

万方数据

(2021)34:58

DOI: 10.1186/s10033-021-00580-5

An Intelligent Fault Diagnosis Method of Multi-Scale Deep Feature Fusion Based on Information Entropy

Zhiwu Shang • Wanxiang Li • Maosheng Gao • Xia Liu • Yan Yu

Abstract: For a single-structure deep learning fault diagnosis model, its disadvantages are an insufficient feature extraction and weak fault classification capability. This paper proposes a multi-scale deep feature fusion intelligent fault diagnosis method based on information entropy. First, a normal autoencoder, denoising autoencoder, sparse autoencoder, and contractive autoencoder are used in parallel to construct a multi-scale deep neural network feature extraction structure. A deep feature fusion strategy based on information entropy is proposed to obtain low-dimensional features and ensure the robustness of the model and the quality of deep features. Finally, the advantage of the deep belief network probability model is used as the fault classifier to identify the faults. The effectiveness of the proposed method was verified by a gearbox test-bed. Experimental results show that, compared with traditional and existing intelligent fault diagnosis methods, the proposed method can obtain representative information and features from the raw data with higher classification accuracy.

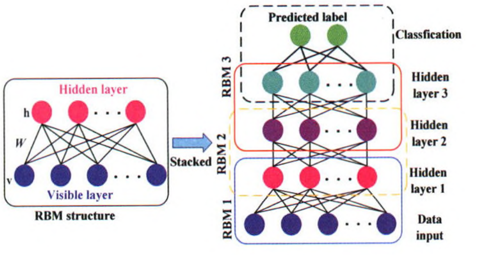

(2021)34:61

DOI: 10.1186/s10033-021-00584-1

A Comparative Study on Asperity Peak Modeling Methods

Wei Zhou • Daiyan Zhao • Jinyuan Tang • Jun Yi

Abstract: The peak identification scheme based method (three-point definition) and the spectral moments based method (spectral moment approach) are both widely used for asperity peak modeling in tribology. To discover the differences between the two methods, a great number of rough surface profile samples with various statistical distributions are first randomly generated using FFT. Then the distribution parameters of asperity peaks are calculated for the generated samples with both methods. The obtained results are compared and verified by experiment. The variation rules of the differences between the two methods with statistical characteristics of rough surfaces are investigated. To explain for the discovered differences, the assumptions by spectral moment approach that the joint distribution of surface height, slope and curvature is normal and that the height distribution of asperities is Gaussian, are examined. The results show that it is unreasonable to assume a joint normal distribution without inspecting the correlation pattern of $[z]$, $[z']$ and $[z'']$, and that the height distribution of asperities is not exactly Gaussian before correlation length of rough surface increases to a certain extent, 20 for instance.

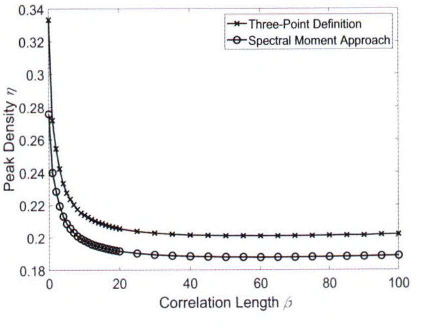

万方数据

CONTENTS

Vol. 34, No. 4, August, 2021

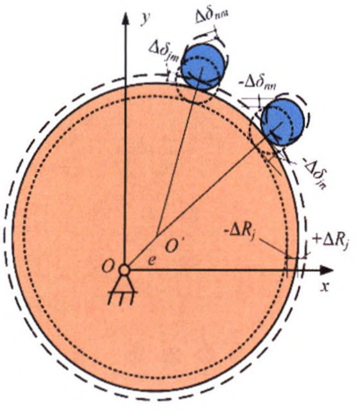

(2021)34:84
DOI: 10.1186/s10033-021-00607-x

Mesh Force Modelling and Parametric Studies for Compound Oscillatory Roller Reducer

Changxu Wei • Chaosheng Song • Caichao Zhu • Chengcheng Liang • Long Hu

Abstract: A compound oscillatory roller reducer (CORR) with a first-stage gear transmission and a second-stage oscillatory roller transmission is presented. The transmission principle of oscillatory roller transmission is introduced, and the tooth profile equation of the inner gear is derived. The analytical model of mesh force considering the installation errors and manufacturing errors is proposed. Then, parametric studies considering different errors on the mesh force are conducted. Results show that the design parameters are significant factors for mesh force. The mesh force is reduced by 17% as the eccentricity of disk cam increases from 2.5 mm to 4 mm. When the radius of the movable roller increases from 7 mm to 20 mm, the mesh force decreases by 8%. As the radius of disk cam increases from 125 mm to 170 mm, the mesh force is decreased by 26.5%. For the impacts of errors, the mesh force has a noticeable fluctuation when these errors exist including the manufacturing error of disk cam, the installation error of disk cam and the manufacturing error of movable roller change. The prototype of the reducer is manufactured and preliminary run-in test proved the feasibility of the transmission principle.

Advanced Transportation Equipment

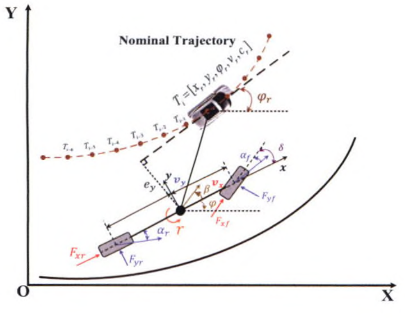

(2021)34:74
DOI: 10.1186/s10033-021-00590-3

Comparative Study of Trajectory Tracking Control for Automated Vehicles via Model Predictive Control and Robust H-infinity State Feedback Control

Kai Yang • Xiaolin Tang • Yechen Qin • Yanjun Huang • Hong Wang • Huayan Pu

Abstract: A comparative study of model predictive control (MPC) schemes and robust H_∞ state feedback control (RSC) method for trajectory tracking is proposed in this paper. The main objective of this paper is to compare MPC and RSC controllers' performance in tracking predefined trajectory under different scenarios. MPC controller is designed based on the simple longitudinal-yaw-lateral motions of a single-track vehicle with a linear tire, which is an approximation of the more realistic model of a vehicle with double-track motion with a non-linear tire mode. RSC is designed on the basis of the same method as adopted for the MPC controller to achieve a fair comparison. Then, three test cases are built in CarSim-Simulink joint platform. Specifically, the verification test is used to test the tracking accuracy of MPC and RSC controller under well road conditions. Besides, the double lane change test with low road adhesion is designed to find the maximum velocity that both controllers can carry out while guaranteeing stability. Furthermore, an extreme curve test is built where the road adhesion changes suddenly, in order to test the performance of both controllers under extreme conditions. Finally, the advantages and disadvantages of MPC and RSC under different scenarios are also discussed.

万方数据

(2021)34:79

DOI: 10.1186/s10033-021-00600-4

An Adaptive Nonsingular Fast Terminal Sliding Mode Control for Yaw Stability Control of Bus Based on STI Tire Model

Xiaoqiang Sun • Yujun Wang • Yingfeng Cai • Pak Kin Wong • Long Chen

Abstract: Due to the bus characteristics of large quality, high center of gravity and narrow wheelbase, the research of its yaw stability control (YSC) system has become the focus in the field of vehicle system dynamics. However, the tire nonlinear mechanical properties and the effectiveness of the YSC control system are not considered carefully in the current research. In this paper, a novel adaptive nonsingular fast terminal sliding mode (ANFTSM) control scheme for YSC is proposed to improve the bus curve driving stability and safety on slippery roads. Firstly, the STI (Systems Technologies Inc.) tire model, which can effectively reflect the nonlinear coupling relationship between the tire longitudinal force and lateral force, is established based on experimental data and firstly adopted in the bus YSC system design. On this basis, a more accurate bus lateral dynamics model is built and a novel YSC strategy based on ANFTSM, which has the merits of fast transient response, finite time convergence and high robustness against uncertainties and external disturbances, is designed. Thirdly, to solve the optimal allocation problem of the tire forces, whose objective is to achieve the desired direct yaw moment through the effective distribution of the brake force of each tire, the robust least-squares allocation method is adopted. To verify the feasibility, effectiveness and practicality of the proposed bus YSC approach, the TruckSim-Simulink co-simulation results are finally provided. The co-simulation results show that the lateral stability of bus under special driving conditions has been significantly improved. This research proposes a more effective design method for bus YSC system based on a more accurate tire model.

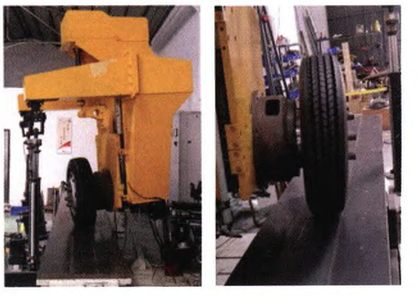

(2021)34:70

DOI: 10.1186/s10033-021-00585-0

Optimisation Method for Determination of Crack Tip Position Based on Gauss-Newton Iterative Technique

Bing Yang • Zhanjiang Wei • Zhen Liao • Shuwei Zhou • Shoune Xiao • Tao Zhu • Guangwu Yang • Mingmeng Wang

Abstract: In the digital image correlation research of fatigue crack growth rate, the accuracy of the crack tip position determines the accuracy of the calculation of the stress intensity factor, thereby affecting the life prediction. This paper proposes a Gauss-Newton iteration method for solving the crack tip position. The conventional linear fitting method provides an iterative initial solution for this method, and the preconditioned conjugate gradient method is used to solve the ill-conditioned matrix. A noise-added artificial displacement field is used to verify the feasibility of the method, which shows that all parameters can be solved with satisfactory results. The actual stress intensity factor solution case shows that the stress intensity factor value obtained by the method in this paper is very close to the finite element result, and the relative error between the two is only −0.621%; the Williams coefficient obtained by this method can also better define the contour of the plastic zone at the crack tip, and the maximum relative error with the test plastic zone area is −11.29%. The relative error between the contour of the plastic zone defined by the conventional method and the area of the experimental plastic zone reached a maximum of 26.05%. The crack tip coordinates, stress intensity factors, and plastic zone contour changes in the loading and unloading phases are explored. The results show that the crack tip change during the loading process is faster than the change during the unloading process; the stress intensity factor during the unloading process under the same load condition is larger than that during the loading process; under the same load, the theoretical plastic zone during the unloading process is higher than that during the loading process.

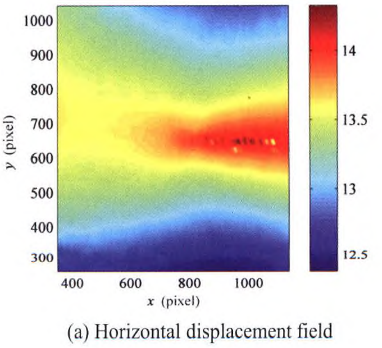

(a) Horizontal displacement field

CONTENTS

Vol. 34, No. 4, August, 2021

(2021)34:86
DOI: 10.1186/s10033-021-00604-0

Optimization on the Crosswind Stability of Trains Using Neural Network Surrogate Model

Le Zhang • Tian Li • Jiye Zhang • Ronghuan Piao

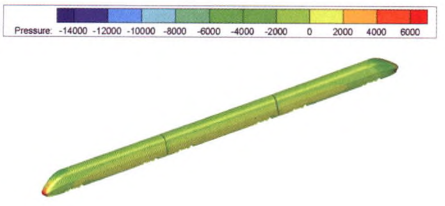

Abstract: Under the influence of crosswinds, the running safety of trains will decrease sharply, so it is necessary to optimize the suspension parameters of trains. This paper studies the dynamic performance of high-speed trains under crosswind conditions, and optimizes the running safety of train. A computational fluid dynamics simulation was used to determine the aerodynamic loads and moments experienced by a train. A series of dynamic models of a train, with different dynamic parameters were constructed, and analyzed, with safety metrics for these being determined. Finally, a surrogate model was built and an optimization algorithm was used upon this surrogate model, to find the minimum possible values for: derailment coefficient, vertical wheel-rail contact force, wheel load reduction ratio, wheel lateral force and overturning coefficient. There were 9 design variables, all associated with the dynamic parameters of the bogie. When the train was running with the speed of 350 km/h, under a crosswind speed of 15 m/s, the benchmark dynamic model performed poorly. The derailment coefficient was 1.31. The vertical wheel-rail contact force was 133.30 kN. The wheel load reduction rate was 0.643. The wheel lateral force was 85.67 kN, and the overturning coefficient was 0.425. After optimization, under the same running conditions, the metrics of the train were 0.268, 100.44 kN, 0.474, 34.36 kN, and 0.421, respectively. This paper show that by combining train aerodynamics, vehicle system dynamics and many-objective optimization theory, a train's stability can be more comprehensively analyzed, with more safety metrics being considered.

Mechanism and Robotics

(2021)34:76
DOI: 10.1186/s10033-021-00595-y

Design of 3D-printed Cable Driven Humanoid Hand Based on Bidirectional Elastomeric Passive Transmission

Teru Chen • Xingwei Zhao • Guocai Ma • Bo Tao • Zhouping Yin

Abstract: Motion control of the human hand is the most complex part of the human body. It has always been a challenge for a good balance between the cost, weight, responding speed, grasping force, finger extension, and dexterity of prosthetic hand. To solve these issues, a 3D-printed cable driven humanoid hand based on bidirectional elastomeric passive transmission (BEPT) is designed in this paper. A semi-static model of BEPT is investigated based on energy conservation law to analyze the mechanical properties of BEPT and a dynamical simulation of finger grasping is conducted. For a good imitation of human hand and an excellent grasping performance, specific BEPT is selected according to human finger grasping experiments. The advantage of BEPT based humanoid hand is that a good balance between the price and performance of the humanoid hand is achieved. Experiments proved that the designed prosthetic hand's single fingertip force can reach 33 N and the fastest fingertip grasping speed realized 0.6 s/180°. It also has a good force compliance effect with only 430g's weight. It can not only grab fragile objects like raw eggs and paper cup, but also achieve strong grasping force to damage metal cans. This humanoid hand has considerable application prospects in artificial prosthesis, human-computer interaction, and robot operation.

万方数据

(2021)34:77

DOI: 10.1186/s10033-021-00594-z

Design of a Flexible Capture Mechanism Inspired by Sea Anemone for Non-cooperative Targets

Jiankun Yang • Chengwei Ren • Chenghao Yang • Youyu Wang • Shumin Wan • Rongjie Kang

Abstract: Robotic grippers have been used in industry as end-effectors but are usually limited to operations in pre-defined workspace. However, few devices can capture irregularly shaped dynamic targets in space, underwater and other unstructured environments. In this paper, a novel continuum arm group mechanism inspired by the morphology and motions of sea anemones is proposed. It is able to dissipate and absorb the kinetic energy of a fast moving target in omni-direction and utilize multiple arms to wrap and lock the target without accurate positioning control. Wire-driven actuation systems are implemented in the individual continuum arms, achieving both bending motion and stiffness regulation. Through finite element method, the influence of different configurations of the continuum arm group on the capture performance is analyzed. A robotic prototype is constructed and tested, showing the presented arm group mechanism has high adaptability to capture targets with different sizes, shapes, and incident angles.

Smart Materials

(2021)34:66

DOI: 10.1186/s10033-021-00583-2

Effects of Active Gases on Droplet Transfer and Weld Morphology in Pulsed-Current NG-GMAW of Mild Steel

Guoqiang Liu • Xinhua Tang • Qi Xu • Fenggui Lu • Haichao Cui

Abstract: The current research of narrow-gap gas metal arc welding (NG-GMAW) primarily focuses on improving the sidewall fusion and avoiding the lack-of-fusion defect. However, the high cost and operation difficulty of the methods limit the industrial application. In this study, small amount of active gases CO_2 and O_2 were added into pure argon inert shielding gas to improve the weld formation of pulsed-current narrow-gap gas metal arc welding (NG-GMAW) of mild steel. Their effects on droplet transfer and arc behavior were investigated. A high-speed visual sensing system was utilized to observe the metal transfer process and arc morphology. When the proportion of CO_2, being added into the pure argon shielding gas, changes from 5% to 25%, the metal transfer mode changes from pulsed spray streaming transfer to pulsed projected spray transfer, while it remains the pulsed spray streaming transfer when 2% to 10% O_2 is added. Both CO_2 and O_2 are favorable to stabilizing arc and welding process. O_2 is even more effective than CO_2. However, O_2 is more likely to cause slags on the weld surface, while CO_2 can improve the weld appearance in some sense. The weld surface concavity in NG-GMAW is greatly influenced by the addition of active gas, but the weld width and weld penetration almost keep constant. This study proposes a new method which is beneficial to improving the weld bead formation and welding process stability.

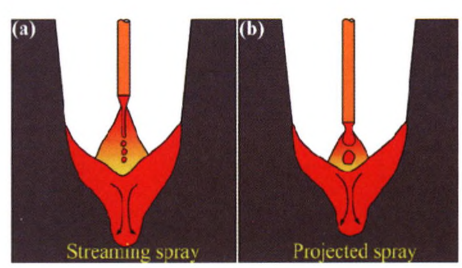

万方数据

CONTENTS

Vol. 34, No. 4, August, 2021

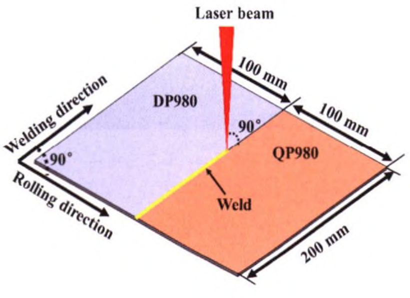

(2021)34:80

DOI: 10.1186/s10033-021-00596-x

HAZ Characterization and Mechanical Properties of QP980-DP980 Laser Welded Joints

Junliang Xue • Peng Peng • Wei Guo • Mingsheng Xia • Caiwang Tan • Zhandong Wan • Hongqiang Zhang • Yongqiang Li

Abstract: The QP980-DP980 dissimilar steel joints were fabricated by fiber laser welding. The weld zone (WZ) was fully martensitic structure, and heat-affected zone (HAZ) contained newly-formed martensite and partially tempered martensite (TM) in both steels. The super-critical HAZ of the QP980 side had higher microhardness (~ 549.5 Hv) than that of the WZ due to the finer martensite. A softened zone was present in HAZ of QP980 and DP980, the dropped microhardness of softened zone of the QP980 and DP980 was Δ 21.8 Hv and Δ 40.9 Hv, respectively. Dislocation walls and slip bands were likely formed at the grain boundaries with the increase of strain, leading to the formation of low angle grain boundaries (LAGBs). Dislocation accumulation more easily occurred in the LAGBs than that of the HAGBs, which led to significant dislocation interaction and formation of cracks. The electron back-scattered diffraction (EBSD) results showed the fraction of LAGBs in sub-critical HAZ of DP980 side was the highest under different deformation conditions during tensile testing, resulting in the failure of joints located at the sub-critical HAZ of DP980 side. The QP980-DP980 dissimilar steel joints presented higher elongation (~ 11.21%) and ultimate tensile strength (~ 1011.53 MPa) than that of DP980-DP980 similar steel joints, because during the tensile process of the QP980-DP980 dissimilar steel joint (~ 8.2% and 991.38 MPa), the strain concentration firstly occurred on the excellent QP980 BM. Moreover, Erichsen cupping tests showed that the dissimilar welded joints had the lowest Erichsen value (~5.92 mm) and the peak punch force (~28.4 kN) due to the presence of large amount of brittle martensite in WZ and inhomogeneous deformation.

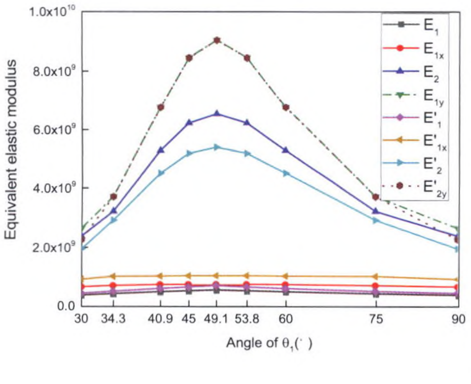

(2021)34:51

DOI: 10.1186/s10033-021-00574-3

Effect of Axial Deformation on Elastic Properties of Irregular Honeycomb Structure

Ning Wang • Qingtian Deng

Abstract: Irregular honeycomb structures occur abundantly in nature and in man-made products, and are an active area of research. In this paper, according to the optimization of regular honeycomb structures, two types of irregular honeycomb structures with both positive and negative Poisson's ratios are presented. The elastic properties of irregular honeycombs with varying structure angles were investigated through a combination of material mechanics and structural mechanics methods, in which the axial deformation of the rods was considered. The numerical results show that axial deformation has a significant influence on the elastic properties of irregular honeycomb structures. The elastic properties of the structure can be considered by the enclosed area of the unit structure, the shape of the unit structure, and the elastic properties of the original materials. The elastic properties considering the axial deformation of rods studied in this study can provide a reference for other scholars.

万方数据

CHINESE JOURNAL OF MECHANICAL ENGINEERING

中国机械工程学报

(Bimonthly, Started in 1988)

Vol. 34, No. 4, August 2021

Supervised by China Association for Science and Technology

Sponsored by Chinese Mechanical Engineering Society

Associated to IFToMM

Chief Editor Tianhu Song

Executive Chief Editor Shuqin Wang

Deputy Chief Editor Dan Liu

Production Editor Yingjiao Xiang

Edited by Editorial Office of Chinese Journal of Mechanical Engineering
Address: 22 Baiwanzhuang Dajie, Beijing 100037, China
Tel: +86-10-88379909
Fax: +86-10-68994557
http: //www.cjmenet.com
E-mail: cjme@cjmenet.com

Printed by Beijing Baochang Color Printing Co., Ltd.

Subscriptions in China Post Offices throughout China
Postal Code: 2-377
Subscription Price in China: ¥ 150

Coverage in Abstracting & Indexing (A&I) Services: Science Citation Index Expanded (SciSearch), Journal Citation Reports/ Science Edition, SCOPUS, DOAJ, INSPEC, Zentralblatt Math, Chemical Abstracts Service (CAS), Google Scholar, CSA, Chinese Science Citation Database, Earthquake Engineering Abstracts, EI-Compendex, OCLC, SCImago, Summon by ProQuest

Online Submission

For enquiries relating to the submission of articles (including electronic submission where available), please visit http: //www.editorialmanager.com/chme, www.cjmenet.com, or cjme.springeropen.com

ISSN 1000-9345

08>

9 771000 934213

万方数据